Chapter 2

Effective Internal Impedance

The impedance boundary condition (IBC) is widely used in scattering problems, eddy current problems, lossy transmission line problems, etc. The IBC is adopted to get rid of the lossy dielectric, multi-layered coatings over conductors in scattering problems, and the lossy conductors in eddy current problems and transmission line problems from the domain to be solved. The problems are solved then by applying the finite element method (FEM) [4, 5], the boundary element method (BEM) [6, 7], the electric/magnetic field integral equation method (MFIE/EFIE) [8, 9], the finite difference time domain method (FDTD) [10, 11], etc. and this IBC reduces the number of unknowns and saves a substantial amount of computation time. But, in general, the boundary condition must be known (at least approximately) *a priori* on the surface, and the accuracy of the fields solved is determined by the relevance of the IBC used.

The most widely used IBC is the Standard Impedance Boundary Condition (SIBC), also called the Leontovich boundary condition [12, 13]. It is valid when the skin depth is small relative to other dimensions of the problem, or the layer is thin and highly lossy. For coated dielectric layers of scatterers, in general, the reflection of electromagnetic wave at the boundary depends on the angle of the incident wave, and it requires higher level of IBCs [13], such as the Tensor Impedance Boundary Condition (TIBC), the Higher Order Impedance Boundary Conditions (HOIBC), etc. For eddy current problems and transmission line problems, the Leontovich boundary condition has been used for lossy conductors at high frequency. In this chapter, as an approximation to the surface impedance of an isolated conductor, three effective internal impedance (EII) models will be presented which approximately characterize the inside of a lossy rectangular conductor from low frequency (i.e., the skin depth is larger than the cross-sectional dimensions of the conductor) to high frequency (i.e., the skin depth is far smaller than the dimensions of the conductor). The effective internal impedance (EII) and SIBC will be compared in the case of rectangular conductors and the appropriateness of the effective internal impedance (EII) models as SIBC will be explained for lossy transmission lines from DC to high frequency.

2.1 Standard Impedance Boundary Condition

Schelkunoff [14] first introduced the concept of surface impedance in electromagnetics in 1934 for the analysis of coaxial cables. And in 1940's Leontovich [12] as well as many other Russians did the basic studies of the surface impedance on a semi-infinite plane of an isotropic linear medium and on a conductor-backed thin lossy dielectric layer where a plane wave is incident. Senior [15] explained in detail the Leontovich boundary conditions and the requisites to be satisfied. According to Leontovich, at the surface on the lossy conductor the electric and magnetic fields are related by

$$\vec{E} - (\hat{n} \cdot \vec{E})\hat{n} = Z_s \hat{n} \times \vec{H} \tag{2.1}$$

where Z_s is the surface impedance and $\hat{n}$ is normal outward unit vector. This SIBC is based on the postulate that the relationship between the tangential electric and magnetic fields at any point on the boundary is a purely local one, depending only on the curvature of the surface and the electromagnetic properties of the bodies. Therefore, the condition of (2.1) is valid only when the curvature radii of the surface is larger than the skin depth, the refractive index of the bodies is larger than that of the external medium and the dimensions of the problem is smaller than the wavelength. That is, the dimensions of the problem are larger than the skin depth, the reflection characteristic is independent of the incident angle, and the operating frequency is much lower than the dielectric relaxation frequency. For a semi-infinite plane of an isotropic linear lossy conductor, the surface impedance is given by

$$Z_S(\omega) = \sqrt{\frac{j\omega\mu}{\sigma}} = \frac{(1+j)}{\sigma\delta} \tag{2.2}$$

where ω is the frequency in radians per second, μ the permeability, σ the conductivity, and δ the skin depth. And for a conductor-backed thin lossy dielectric, the surface impedance is

$$Z_S(\omega) = \sqrt{\frac{j\omega\mu}{\sigma + j\omega\varepsilon}} \tanh\{\gamma(\omega)d\} \tag{2.3}$$

where the propagation constant $\gamma(\omega) = \sqrt{j\omega\mu(\sigma + j\omega\varepsilon)}$, and d is the thickness of the dielectric layer. For geometries having curvature, Leontovich introduced a first order curvature correction term to the surface impedance for small radii of curvature and Mitzner [16] refined it later.

Unless restrictions are placed on the shape of the surface, the IBC should involve the geometrical properties in addition to the curvature, as well as the electrical properties of the material and, in consequence, may vary from point to point on the surface. Many transmission lines make use of conductors with rectangular cross-section, and corners and slots are generally used for eddy current problems such as non-destructive testing (NDT), shielding, etc. Several models for corners and edges [18-20] have been presented for use as an SIBC. Even though those models have been based on profound understandings of electromagnetics, still there is a lack of accuracy at low frequency. And, in addition, for low frequency where the skin depth is comparable to or larger than the dimensions of the structures, the surface impedance has no more the local property and depends on the global geometries of the conductors. At low frequency the surface impedance when other conductors are present considerably differ from the surface impedance of an isolated conductor. These limit the usefulness of SIBC for lossy transmission lines at low frequency and necessitate higher order models of impedance boundary conditions (IBC). In following sections, three models of the effective internal impedance (EII) are introduced for the case of rectangular conductors, which approximates the surface impedance of an isolated conductors and is used to represent resistance and internal inductance of the conductors. These are compared with each other and the surface impedance of the isolated rectangular conductor, and the utilization of EII is clarified compared to SIBC.

2.2 Effective Internal Impedance of Rectangular Conductors

As the speed of the integrated circuits (IC) is getting higher, the loss of the interconnects is becoming more important. The high speed digital signals span a wide bandwidth from DC to frequencies about the inverse of the rise time, and at high frequency the skin and proximity effects begin to take effect. On the other hand in monolithic microwave integrated circuits (MMIC) the miniaturization of the structure causes the conductor loss to increase, and the skin depth is on the order of the size of the conductors. Therefore, fast and efficient methods are needed to evaluate frequency dependent parameters of the lossy transmission lines from DC to high frequency, i.e., resistance and inductance for quasi-TEM transmission lines, which are used for circuit simulations.

The Leontovich boundary condition at low frequency, and at corners and edges of the structure, can be modified in some cases. For a thin flat conductors in an MMIC, instead of a single-valued surface impedance (2.4), the surface impedance matrix (2.5) can be used to relate the tangential electric field of one surface to the tangential magnetic fields of the other surface as well as of the same surface at low frequency. This is called the transfer impedance boundary condition as in reference [17], and under the same incident fields on both sides of the thin flat conductors it becomes (2.4).

$$Z_s(\omega) = \frac{\sqrt{\dfrac{j\omega\mu}{\sigma}}}{\tanh\left\{\sqrt{j\omega\mu\sigma}\,\dfrac{t}{2}\right\}} = \frac{\dfrac{(1+j)}{\sigma\delta}}{\tanh\left\{\dfrac{(1+j)}{\delta}\,\dfrac{t}{2}\right\}} \tag{2.4}$$

where t is the thickness of the conductor.

$$\begin{pmatrix} E_{\parallel}^{t} \\ E_{\parallel}^{b} \end{pmatrix} = \begin{pmatrix} Z_{tt} & Z_{tb} \\ Z_{bt} & Z_{bb} \end{pmatrix} \begin{pmatrix} H_t^{t} \\ H_t^{b} \end{pmatrix} \tag{2.5}$$

where

$$Z_{tt} = Z_{bb} = \frac{\sqrt{\dfrac{j\omega\mu}{\sigma}}}{\tanh\left(\sqrt{j\omega\mu\sigma}\,t\right)} = \frac{\dfrac{(1+j)}{\sigma\delta}}{\tanh\left\{\dfrac{(1+j)}{\delta}\,t\right\}}$$

$$Z_{tb} = Z_{bt} = \frac{\sqrt{\dfrac{j\omega\mu}{\sigma}}}{\sinh\left(\sqrt{j\omega\mu\sigma}\,t\right)} = \frac{\dfrac{(1+j)}{\sigma\delta}}{\sinh\left\{\dfrac{(1+j)}{\delta}\,t\right\}}$$

and $E_{\parallel}^{t}$ and $E_{\parallel}^{b}$, H_t^{t} and H_t^{b} are the electric field parallel to current flows and the tangential magnetic field on the top and the bottom of the plates, respectively. But for rectangular conductors where width to thickness ratio is not too large, the above modification to the surface impedance model must consider all four surfaces, making a 4×4 matrix, with each element of the matrix a complicated, position-dependent function of geometries. For the structures of the interconnects in high speed digital integrated circuits and modern MMICs, rectangular conductors are the common geometries and the thickness is not negligible compared to the width of the conductor.

Deely [18] introduced a modified surface impedance near a 90° corner for analyzing the induction heating problem with BEM. It is based on the assumption that the transverse magnetic (TM) plane wave is normally incident onto all surfaces of the conductor, and this model gives good approximation to the surface impedance from mid to high frequency. Jingguo *et al.* [19, 20] extended this model to corners of arbitrary angle, transverse electric (TE) problems, and three dimensional structures of cubic conductor and cylindrical conductor. But these models only consider the interaction between two adjoining surfaces. This model has been recently modified to consider the effect of all four sides of rectangular conductors for transverse magnetic (TM) problems [21, 22], and is named the plane wave model. This plane wave model still gives poor approximation to the surface impedance at low frequency and in this section the modified model is introduced along with previous works. The surface impedance of the rectangular conductor could be modeled by using a transmission line analogy, and it has been successfully used for analyzing several lossy transmission lines [23]. This transmission line model is also explained in this section. The proposed models are to be used to evaluate resistance and inductance of lossy transmission lines, not to calculate the fields of the problems, but to represent resistance and internal inductance of the lossy conductors. So, to distinguish the proposed models from SIBC these are named the effective internal impedance (EII).

2.2.1 Plane Wave Model

Under the assumption that a transverse magnetic (TM) plane wave is incident onto the surface of the conductors, the surface impedance can be approximated by solving the diffusion equation locally. But this does not give a good approximation at low frequency because this only considers the two adjoining surfaces. By assuming uniform TM plane waves incident on all four surface as shown in Fig. 2.1 and considering the fields penetrating from the other three surfaces, the magnetic and electric field on one surface of the conductor c wide and d thick can be represented, respectively, by

$$\vec{H}(x,y) = H_o\left[\left(e^{-\gamma y} - e^{\gamma(y-d)}\right)\hat{a}_x + \left(-e^{-\gamma x} + e^{\gamma(x-c)}\right)\hat{a}_y\right] \tag{2.6}$$

$$\vec{E}(x,y) = \hat{a}_z H_o \sqrt{\frac{j\omega\mu}{\sigma}}\left(e^{-\gamma x} + e^{\gamma(x-c)} + e^{-\gamma y} + e^{\gamma(y-d)}\right) \tag{2.7}$$

EII is expressed by relating the tangential electric field to the tangential magnetic field,

$$Z_{eii}(\omega, x, y=0) = \frac{E_z}{H_x} = \sqrt{\frac{j\omega\mu}{\sigma}}\,\frac{e^{-\gamma x} + e^{\gamma(x-c)} + 1 + e^{-\gamma d}}{1 - e^{-\gamma d}} \tag{2.8}$$

The equation above is quite simple and closed form approximating the surface impedance of an isolated rectangular conductor. In the limit of $\omega \to 0$, on the top, bottom, and side surfaces this model gives a constant surface impedance, respectively, of

$$Z_{eii}(0, x, y = 0) = \frac{4}{\sigma d} \tag{2.9}$$

$$Z_{eii}(0, x = 0, y) = \frac{4}{\sigma c} \tag{2.10}$$

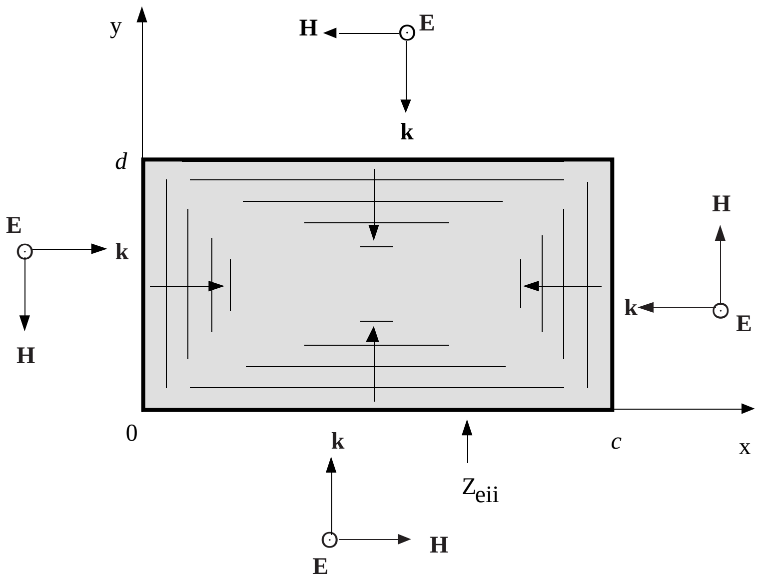

Figure 2.1: Plane wave model for the effective internal impedance. Transverse Magnetic (TM) wave is incident onto all surfaces of the conductor. Effective internal impedance is calculated by solving diffusion equation locally.

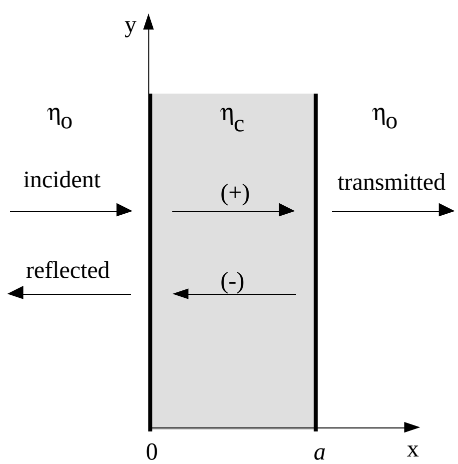

Figure 2.2: Wave reflection and transmission from a lossy conductor in air.

From these constant EII the correct DC resistance is obtained. But all four surfaces share the same amount of resistance, which is a poor approximation to the surface impedance for wide rectangular conductors at low frequency . At high frequency where the skin depth is far smaller than the geometries of the problem, this model approaches $\sqrt{j\omega\mu / \sigma}$, the surface impedance of a semi-infinite plane of an isotropic conductor.

2.2.2 Modified Plane Wave Model

When the skin depth is comparable to or larger than the thickness or width of the conductor, the incident fields onto one surface of the conductor not only penetrate to but also reflect from the interfaces as shown in Fig. 2.2. By allowing this reflection and transmission of the incident field at the interfaces of two media, the magnetic field is expressed by

$$\vec{H}(x,y) = H_o\left\{\hat{a}_x\left[\frac{e^{-\gamma y} - e^{\gamma(y-d)} + \Gamma\left(e^{\gamma(y-2d)} - e^{-\gamma(y+d)}\right)}{1-\Gamma e^{-2\gamma d}}\right]\right.$$
$$\left. +\hat{a}_y\left[\frac{-e^{-\gamma x} + e^{\gamma(x-c)} + \Gamma\left(e^{\gamma(x-2c)} - e^{-\gamma(x+c)}\right)}{1-\Gamma e^{-2\gamma c}}\right]\right\}, \qquad (2.11)$$

where

$$\Gamma = \frac{\eta_o - \eta_m}{\eta_o + \eta_m} \qquad \eta_o = \sqrt{\frac{\mu_o}{\varepsilon_o}} \qquad \eta_m = \sqrt{\frac{j\omega\mu}{\sigma}}.$$

Γ is the reflection coefficient at the interface between the conductor and air (seen from conductor side), and η_o and η_m are wave impedances of air and conductor, respectively. The electric field is given by

$$\vec{E}(x,y)=\hat{a}_z H_o\sqrt{\frac{j\omega\mu}{\sigma}}\left\{\frac{e^{-\gamma y}+e^{\gamma(y-d)}+\Gamma\left(e^{\gamma(y-2d)}+e^{-\gamma(y+d)}\right)}{1-\Gamma e^{-2\gamma d}}\right.$$
$$\left.+\frac{e^{-\gamma x}+e^{\gamma(x-c)}+\Gamma\left(e^{\gamma(x-2c)}+e^{-\gamma(x+c)}\right)}{1-\Gamma e^{-2\gamma c}}\right\}. \qquad (2.12)$$

Therefore, a modified plane wave model EII is written at a point on the bottom or top surface as

$$Z_{eii}(\omega,x,y=0)=\sqrt{\frac{j\omega\mu}{\sigma}}\frac{1}{\left(1-e^{-\gamma d}\right)\left(1+\Gamma e^{-\gamma d}\right)}\left\{\left(1+e^{-\gamma d}\right)\left(1+\Gamma e^{-\gamma d}\right)\right.$$
$$\left.+\frac{1-\Gamma e^{-2\gamma d}}{1-\Gamma e^{-2\gamma c}}\left[e^{-\gamma x}+e^{\gamma(x-c)}+\Gamma\left(e^{\gamma(x-2c)}+e^{-\gamma(x+c)}\right)\right]\right\} \qquad (2.13)$$

As $\omega \to 0$, above model gives constant EII for all surfaces,

$$Z_{eii}\left(0,x=0,y\right)=Z_{eii}\left(0,x,y=0\right)=\frac{2}{\sigma}\left(\frac{1}{c}+\frac{1}{d}\right). \qquad (2.14)$$

This gives the right DC resistance, and averages DC resistance over all the surface with uniform weighting. At high frequency this model also approaches to $\sqrt{j\omega\mu/\sigma}$, the surface impedance of a semi-infinite plane of an isotropic conductor.

2.2.3 Transmission Line Model

A simple expression of EII for the case of a rectangular conductor with appreciable ratio of thickness to width is to divide the conductor into segments as in Fig. 2.3. At low frequency the rectangular conductor is segmented into four square corners and two flat rectangular sections as in Fig. 2.3(a). At high frequency, current crowds towards the surface of the conductor to within a few skin depths, and the position dependence of the surface impedance is confined within above a 3δ distance from the corner. Therefore, as shown in Fig. 2.3(b) at high frequency the rectangular

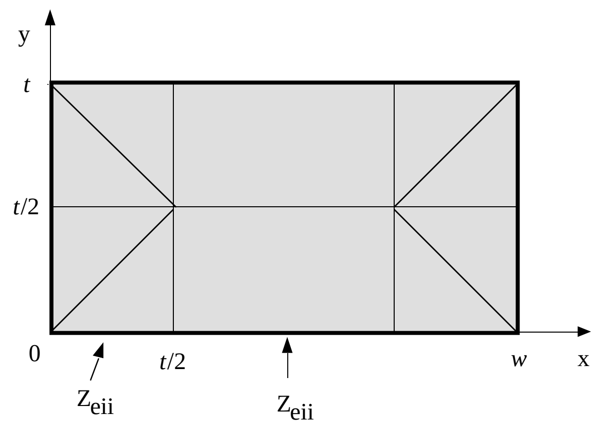

(a) At frequencies of $t/2 < 3\delta$.

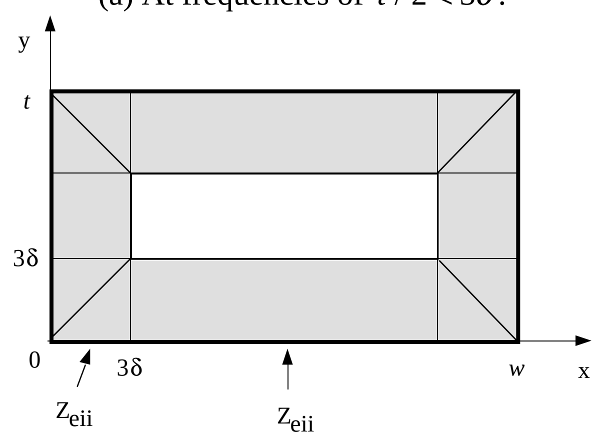

(b) At frequencies of $t/2 > 3\delta$. A rectangular conductor is modeled by a rectangular pipe with thickness of 3δ.

Figure 2.3: Transmission line model for the effective internal impedance. A rectangular conductor is segmented into flat rectangles and four squares. The effective internal impedance is calculated from transverse resonance method and telegraphist's equations.

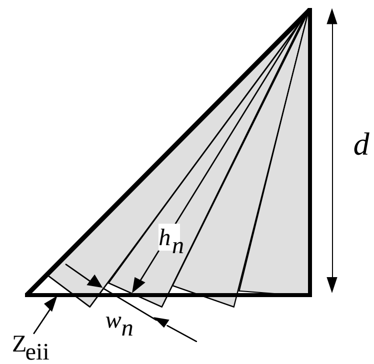

Figure 2.4: Each right-angled triangle is segmented into several isosceles triangles to take care of current crowding towards the corner. Effective internal impedance is calculated from transverse resonance method and telegraphist's equations of non-uniform transmission lines.

conductor is modeled by a hollow rectangular pipe and segmented into four square corners and four flat rectangular sections. By symmetry the square corner is divided into two right-angled triangles.

For the central flat rectangular sections, EII is given by (2.4) where $t/2$ can be replaced by 3δ if $t/2 > 3\delta$. As frequency goes up current crowds more towards corners and to capture this effect a triangular section is divided into N isosceles as shown in Fig. 2.4. For each isosceles h_n is used as the "thickness" of that segment, which is the distance from the center of the base to the opposite corner. And the width of that segment is given in order to trace a wave propagation from the base to the opposite corner. For the n^{th} (n=0, 1, 2,..., $N-1$) segment, the height h_n is given by

$$h_n = d\sqrt{1+\left(\frac{n+0.5}{N}\right)^2} \tag{2.15}$$

and the width w_n by

$$w_n = \frac{h_n}{2}\left[\frac{1}{N+(n+0.5)\frac{n}{N}} + \frac{1}{N+(n+0.5)\frac{n+1}{N}}\right] \tag{2.16}$$

And the surface impedance is approximated by applying transverse resonance and non-uniform transmission line analysis. The total input impedance is obtained for a triangular transmission line with width w_n at the input end, plate separation of unit distance and length h_n, and filled with a uniform conducting material of conductivity σ. Therefore, EII is given through normalizing the input impedance of the triangular transmission line by the width of the original base d / N

$$Z_{eii}^n = \frac{j\sqrt{j\omega\mu\sigma}}{\sigma}\frac{J_0\left(j\sqrt{j\omega\mu\sigma}h_n\right)}{J_1\left(j\sqrt{j\omega\mu\sigma}h_n\right)}\frac{d}{w_n N}, \tag{2.17}$$

where J_0 and J_1 are the Bessel functions of the first kind.

2.3 Comparisons of Three Effective Internal Impedance Models

Three EII models are compared with each other and to the surface impedance for a rectangular conductor 20 μm wide and 4 μm thick in Fig. 2.5, where all models and the surface impedance are normalized by the surface impedance of a flat conductor (2.4). In Fig. 2.5(a) at the frequency such that the skin depth $\delta = 5t$, the plane wave model gives an almost constant EII over each surface, but scaled relative to each other by the ratio of width to thickness (as seen in (2.9) and (2.10)). This model deviates the most among three models from the actual surface impedance. The modified plane wave model gives a constant EII for all sides and is fairly close to the surface impedance except near the corners. The transmission line model well approximates the surface impedance at corners of the wide side, but is off from the surface impedance on the other corner. Figure 2.5(b) shows the comparison at the frequency such that $\delta = t / 2$. Unlike the case of low frequency both plane wave models asymptotically approach the surface impedance. And transmission line model also approaches the surface impedance with some deviation near the corners. Beyond a distance of 3δ from the corner all models are the same as the surface impedance of flat wide conductors. As shown in Fig. 2.5(c) at a high frequency such that $\delta = t / 6$ all models follow the surface impedance. The plane wave model and modified plane wave model become identical and get closer to the surface impedance, and transmission line model is also close to the surface impedance. Again, beyond a distance of 3δ from the corner all models and the actual surface impedance give a constant value. Thus over the whole frequency band the modified plane wave model gives an EII closest to the surface impedance, the transmission line model also gives an EII quite close to the surface impedance, and the plane wave model gives an EII that has the greatest error at low frequency, but becomes identical to the modified plane wave model at high frequency.

Even though the EII models tend to approximate the surface impedance, this is not actually a necessary condition. The usefulness of EII in analyzing the lossy transmission line lies in the accuracy of the line parameters, i.e., resistance and inductance. At high frequency all models approach the surface impedance and the Leontovich boundary condition is valid. Therefore, as shown in Fig. 2.5(c) all models can substitute for the surface impedance and be used as a SIBC. At low frequency all models and the surface impedance give the right DC resistance. Another metric to measure the usefulness of an EII model is the low frequency inductance, which con

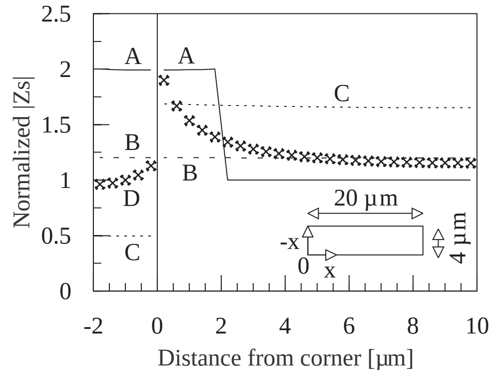

(a) At the frequency of $\delta = 5t$

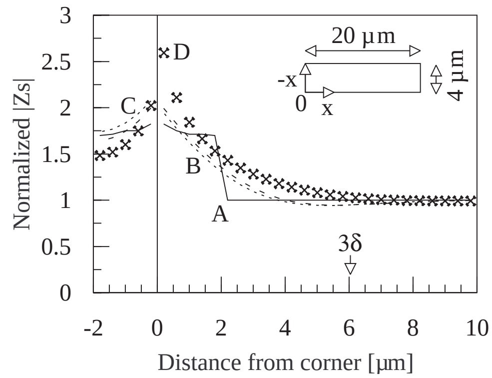

(b) At the frequency of $\delta = t/2$

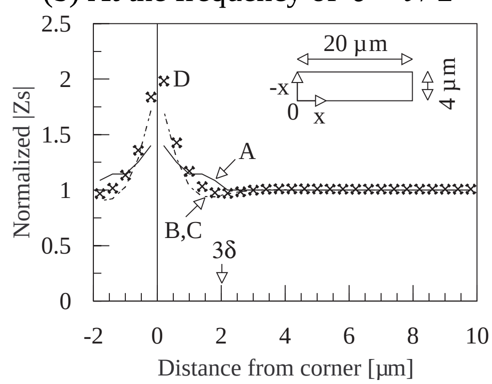

(c) At the frequency of $\delta = t/6$

Figure 2.5: Comparison between three effective internal impedance models and the surface impedance for a rectangular conductor at $\delta = 5t$, $\delta = t/2$, and $\delta = t/6$ (20 μm wide, and 4 μm thick). A(solid line): transmission line model; B(dashed line): modified plane wave model; C(dotted line): plane wave model; D(×): the surface impedance calculated by the volume filament method [24].

sists of internal inductance and external inductance. To calculate the inductance the EII must be incorporated with the external field solvers as a SIBC. Among various formulations describing electromagnetic fields, the current integral equation has successfully been combined with EII to evaluate the series impedance of the lossy transmission lines. This approach is called the surface ribbon method [21, 22] and will be explained in Chapter Four. At low frequency EII determines the current distribution in the surface ribbon method, and affects internal inductance and external inductance. In the surface ribbon method the internal inductance is given by

$$L_{\text{int}} = \lim_{\omega \to 0} \frac{1}{|I|^2} \left\{ \frac{1}{\omega} \oint_S \text{Im}\{Z_{eii}(\omega)\} |J_s|^2 \, dl - \oint_S \left(\vec{A} \times \vec{H}^*_{in} \right) \cdot \hat{n} dl \right\} \tag{2.18}$$

where I is the total current, S is the surface of the conductor, J_s the surface current, $\vec{A}$ the magnetic vector potential, $\vec{H}_{in}$ the magnetic field intensity on the inner surface of the conductor, and $\hat{n}$ normal outward unit vector. In the above equation the second term is small compared to the first term in case of an isolated conductor, which is used to approximate the magnetic energy stored inside the conductor together with EII. It also becomes negligible as width to thickness ratio increases. Figure 2.6 shows the comparison of normalized DC internal inductance and normalized total DC inductance with different EII models. For the convenience the inductance as $\omega \to 0$ is defined as "DC inductance". These are also compared to a more rigorous quasi-TEM volume filament technique [24], where the internal inductance is calculated using

$$L_{\text{int}} = \frac{1}{|I|^2} \int_{v_c} \mu_o \vec{H} \cdot \vec{H}^* \, dv = L_{total} - \oint_S \left(\vec{A} \times \vec{H}^* \right) \cdot \hat{n} dl, \tag{2.19}$$

where v_c is the volume inside the conductor. For a square conductor all models give accurate internal inductance and total inductance. But as the ratio of width to thickness increases, the internal inductance with the plane wave model diverges, causing a large amount of error in the total DC inductance. The modified plane wave model and transmission line model give an internal inductance close to the internal inductance calculated by the volume filament method over the range of width to thickness ratio shown (less than 1% error from the result of the volume filament method).

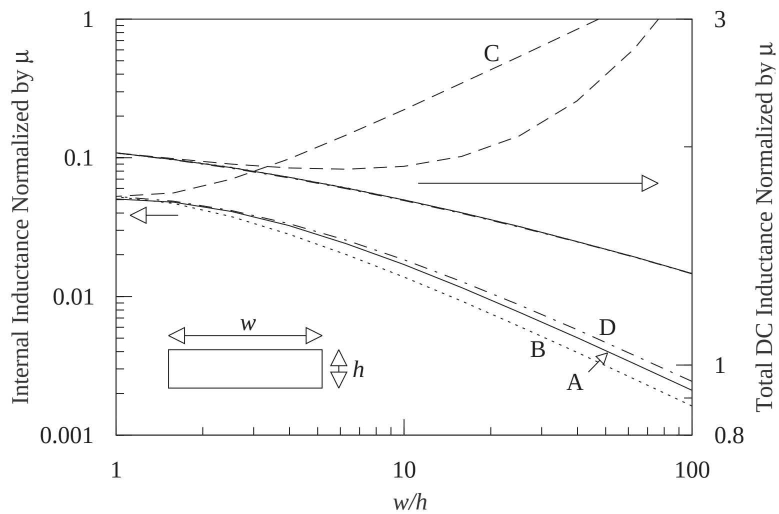

Figure 2.6: Comparison of DC internal inductance and total DC inductance with different effective internal impedance models in conjunction with the surface ribbon method [21, 22] for *w/h* ratio of 1 to 100. These are compared to each other and the results of the volume filament method [24]. A(solid line): volume filament method; B(dotted line): transmission line model; C(dashed line): plane wave model; D(dot-and-dashed line): modified plane wave model.

In summary, at low frequency the modified plane wave model and transmission line model both give accurate resistance and inductance from square to wide rectangular conductors when used in conjunction with the surface ribbon method. And at high frequency all models approach the correct surface impedance.

2.4 Application of Effective Internal Impedance in Lossy Transmission Line Analysis

For lossy transmission lines, fast and efficient methods for resistance and inductance computation can be obtained in conjunction with the use of an EII. Among various electromagnetic field solvers, BEM is examined here using EII as a SIBC. Poor results of BEM using EII as a SIBC at low frequency force the use of external field solvers with EII, such as surface ribbon method [21, 22], which will be discussed in Chapter Four.

2.4.1 Boundary Element Method with the Standard Impedance Boundary Condition

BEM is widely used in analyzing eddy current problems and transmission line problems. Also in BEM SIBC eliminates the conducting region, reduces the number of unknowns, and makes the problem simpler. There have been several efforts applying SIBC in BEM for eddy current problems, but many of them are valid only at high frequency, although some surface impedance models were extended to mid frequency range. If the proposed EII could be used for SIBC, then SIBC could be extended to low frequency regime.

From Maxwell's equations and Green's theorem, the coupled integral equations [25] are set up at the surface of the conductor;

$$\int_{\Gamma} dr' G_o^1(r,r') j\omega\mu H_t(r') - \int_{\Gamma} dr' \left[G_o^2(r,r') - 0.5\delta(r-r') \right] \left(E_z(r') + \nabla\Phi \right) = 0$$

$$\int_{\Gamma} dr' G_c^1(r,r') j\omega\mu H_t(r') - \int_{\Gamma} dr' \left[G_c^2(r,r') + 0.5\delta(r-r') \right] E_z(r') = 0 \qquad (2.20)$$

$$\int_{\Gamma} dr' H_t(r') = I_q,$$

where

$$G_o^1(r,r') = -\frac{1}{2\pi} \ln|r-r'|$$

$$G_c^1(r,r') = -\frac{j}{4} H_0^{(2)}\left(\gamma|r-r'|\right)$$

and Γ is the surface of the conductor, $G_o^2(r,r')$ and $G_c^2(r,r')$ are the derivatives of $G_o^1(r,r')$ and $G_c^1(r,r')$ with respect to normal outward unit vector, Φ is the applied potential, I_q is total current in the q^{th} conductor, $H_0^{(2)}$ the Hankel function of the second kind, and $\delta(r-r')$ is the Dirac delta function. By applying IBC equation (2.20) is simplified to

$$\int_{\Gamma} dr' \left\{ j\omega\mu G_o^1(r,r') - Z_s(r') \left[G_o^2(r,r') - 0.5\delta(r-r') \right] \right\} H_t(r')$$

$$- \int_{\Gamma} dr' \left[G_o^2(r,r') - 0.5\delta(r-r') \right] \nabla\Phi = 0 \qquad (2.21)$$

$$\int_{\Gamma} dr' H_t(r') = I_q .$$

In addition to reducing the number of unknowns by half, SIBC avoids the computation of the Bessel functions.

As shown in Fig. 2.7(a) in the case of a circular conductor BEM (full BEM) and BEM combined with SIBC (surface BEM) give almost identical resistance and inductance over the entire frequency range, except low frequency inductance calculated using full BEM. Full BEM has numerical difficulties in calculating low frequency inductance, when the current is uniform and the normal derivative becomes small. The surface impedance of a circular conductor is given by

$$Z_s = \frac{j\sqrt{j\omega\mu\sigma}}{\sigma}\frac{J_0\left(jr\sqrt{j\omega\mu\sigma}\right)}{J_1\left(jr\sqrt{j\omega\mu\sigma}\right)}, \tag{2.22}$$

where *r* is the radius of the circular conductor. For twin circular conductors in Fig.2.7(b) full BEM and surface BEM using two surface impedance models as the SIBC are compared. The surface impedance of an isolated circular conductor, (2.22), and the actual surface impedance calculated using BEM when the twin circular conductors are closely coupled are used as SIBC. Using the actual surface impedance surface BEM and full BEM give the same results. And using the surface impedance of an isolated circular conductor high frequency resistance and inductance match well to full BEM, but low frequency inductance agreement is poor: compared to full BEM, the error is about 17%. Also low and mid frequency resistance agreement is poor, with about 12% deviation from full BEM.

As shown in Fig. 2.8(a) in the case of a single rectangular conductor BEM combined with the surface impedance calculated by the volume filament technique, EII of the transmission line model, and EII of the modified plane wave model give fairly accurate resistance and inductance over the entire frequency range. High frequency resistance and inductance approach the results of BEM. But mid frequency resistance using the transmission line model for EII deviates by 11%, while low frequency inductance is calculated with less than 1% error. For the coupled conductors in Fig. 2.8(b) high frequency resistance and inductance match well to full BEM, and surface BEM using the actual surface impedance give the same results to full BEM for all frequency range. But low frequency inductance agreement is poor, when EII models are

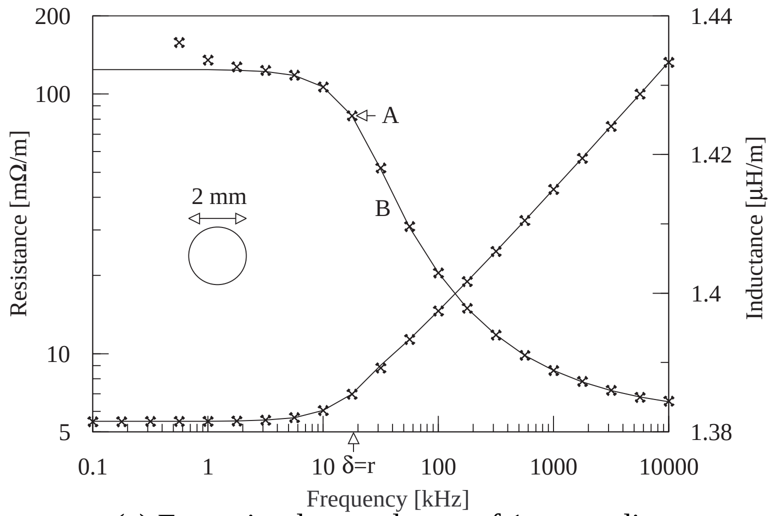

(a) For a circular conductor of 1 mm radius

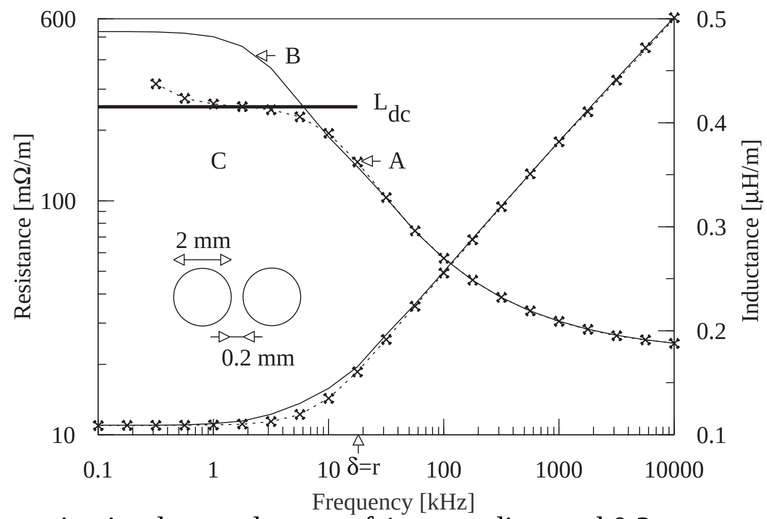

(b) For twin circular conductors of 1 mm radius, and 0.2 mm separation

Figure 2.7: Comparison of resistance and inductance between boundary element method without the standard impedance boundary condition (full BEM) and boundary element method with the standard impedance boundary condition (surface BEM). A(×): BEM without SIBC; B(solid line): BEM with the surface impedance of isolated conductor as SIBC; C(dashed line): BEM with the surface impedance of twin coupled conductors as SIBC, which is calculated by the boundary element method. The conductor surface is divided into 90 uniform elements. The conductivity is 5.8×10^7 [S/m].

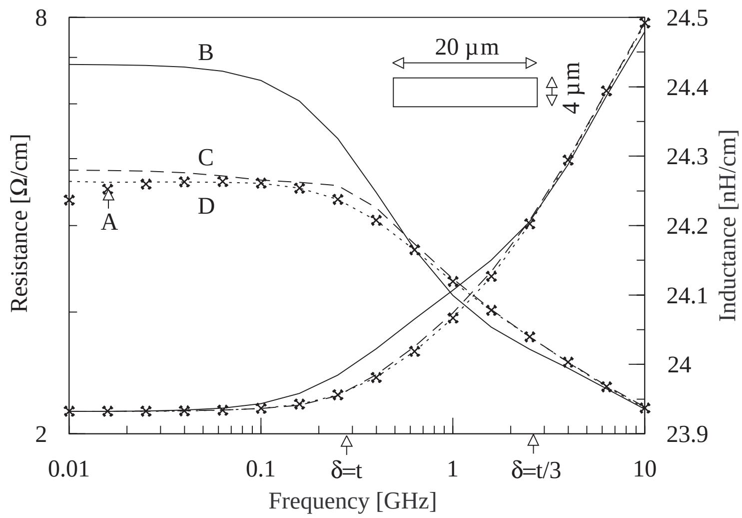

(a) For a rectangular conductor of 20 µm wide and 4 µm thick

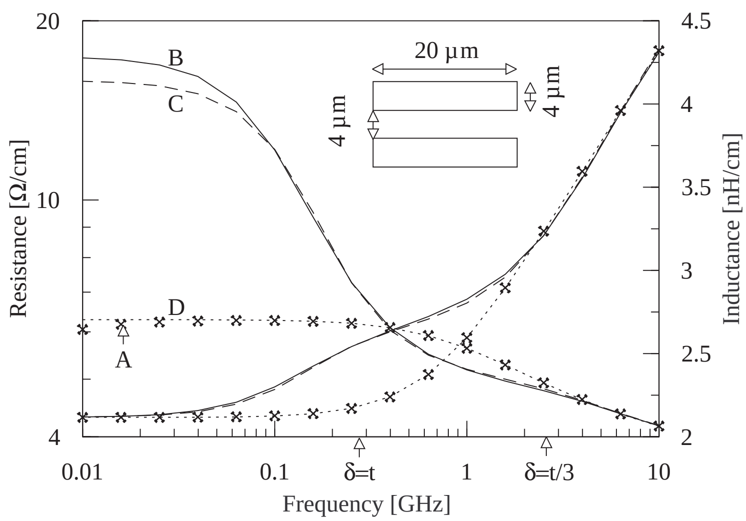

(b) For twin rectangular conductors of 20 µm wide, 4 µm thick, and 4 µm gap

Figure 2.8: Comparison of resistance and inductance between boundary element method without the standard impedance boundary condition (full BEM) and boundary element method with the standard impedance boundary condition (surface BEM). A(×): BEM without SIBC; B(solid line): BEM with transmission line model as SIBC; C(dashed line): BEM with modified plane wave model as SIBC; D(dotted line): BEM with the surface impedance as SIBC, which is calculated by the volume filament method [24]. The conductivity is 5.8×10^{7} [S/m].

Problem	Method	Number of unknowns	CPU time[sec/frequency] Assembling	Solving
Single Conductor	BEM	145	62.3	1.19
	BEM/SIBC	73	0.05	0.15
Twin Conductor	BEM	290	126.12	6.88
	BEM/SIBC	145	0.23	1.19

Table 2.1: Comparison of run time on an IBM RISC 6000 for boundary element method with the standard impedance boundary condition (SIBC) and without the standard impedance boundary condition (SIBC). BEM with SIBC is at least 100 times faster than BEM in assembling a matrix, and at least 5 times in solving the matrix with gaussian elimination algorithm.

used: compared to BEM, the error is 58% and 53% for transmission line model and modified plane wave model, respectively. Mid frequency resistance agreement is also poor when EII models are used, with about 30% deviation from full BEM. Table 2.1 shows the gain using SIBC in computational time on an IBM RISC 6000.

2.4.2 Boundary Element Method assuming Impedance Sheet carrying Surface Current on the Conductor Surface

BEM using SIBC converts a multi-media problem to a one medium, exterior problem, where the surface impedance is used as a relating factor between tangential components of exterior magnetic and electric fields, and the conductor interior is excluded from the domain to be solved. But accurately modeling the surface impedance becomes complicated at low and mid frequency especially for multi-conductor lines. Thus, the usefulness of SIBC is limited at low and mid frequency.

Instead of developing higher order IBC models to capture the non-localized fields at low frequency, a conductor is modeled as an impedance sheet on the conductor surface. The surface current is defined and the conductor interior is regarded as exterior material. Therefore, the coupled integral equations, (2.20), are modified to

$$\int_{\Gamma} dr' G_o^1(r,r') j\omega\mu H_t^{out}(r') - \int_{\Gamma} dr' \left[G_o^2(r,r') - 0.5\delta(r-r')\right]\left(E_z^{out}(r') + \nabla\Phi\right) = 0$$

$$\int_{\Gamma} dr' G_o^1(r,r') j\omega\mu H_t^{in}(r') - \int_{\Gamma} dr' \left[G_o^2(r,r') + 0.5\delta(r-r')\right]\left(E_z^{in}(r') + \nabla\Phi\right) = 0 \,. \quad (2.29)$$

The electric fields are continuous at the impedance sheet. EII is used as relating factor between tangential electric field and the difference of tangential magnetic fields in and out of the impedance sheet as

$$Z_{eii} = \frac{E_z}{H_t^{out} - H_t^{in}} = \frac{E_z}{J_s} \,. \quad (2.30)$$

By applying above condition and for three-dimensional, free space Green's function, the integral equation (2.29) becomes

$$Z_{eii}(r) J_s(r) + \frac{j\omega\mu}{4\pi} \int_{\Gamma} dr' \frac{J_s(r')}{|r-r'|} = -\nabla\Phi \quad (2.31)$$

This equation is the same formula of the surface ribbon method (SRM), one of the successful techniques using EII to accurately and efficiently calculate frequency dependent resistance and inductance of lossy transmission lines. This approach is explained in Chapter Four.

2.4.3 Other External Field Solvers

As shown above BEM using SIBC is not a proper approach to evaluate the series impedance of lossy transmission lines at low and mid frequency. Many other methods, such as the finite element method (FEM), the finite difference time domain method (FDTD), etc., would give the same results, because all of these would use EII as the standard impedance boundary condition (SIBC) and SIBC eliminates the conductor interior from the domain of problem. However, if the conductor is modeled as an impedance sheet on the conductor surface, the conductor interior is replaced as the conductor exterior, and the conductor interior is included in the domain of problem, then those methods would give accurate results using appropriate impedance factors. If EII could be used for characterizing the conductor interior, it would save a lot of computational time without loss in accuracy for the series impedance calculation of lossy transmission lines. The following chapters will explain the conformal mapping technique and current ribbon method as the external field solvers incorporated with EII.